Am. J. Hum. Genet. 76:804–814, 2005

A Novel *STX16* Deletion in Autosomal Dominant Pseudohypoparathyroidism Type Ib Redefines the Boundaries of a *cis*-Acting Imprinting Control Element of *GNAS*

Agnès Linglart,[1] Robert C. Gensure,[3] Robert C. Olney,[4] Harald Jüppner,[1,2] and Murat Bastepe[1]

[1]Endocrine Unit, Department of Medicine, and [2]Pediatric Nephrology Unit, MassGeneral Hospital *for* Children, Massachusetts General Hospital and Harvard Medical School, Boston; [3]Department of Pediatrics, Tulane University School of Medicine, New Orleans; and [4]Nemours Children's Clinic and Mayo Medical School, Jacksonville, FL

A unique heterozygous 3-kb microdeletion within *STX16*, a closely linked gene centromeric of *GNAS*, was previously identified in multiple unrelated kindreds as a cause of autosomal dominant pseudohypoparathyroidism type Ib (AD-PHP-Ib). We now report a novel heterozygous 4.4-kb microdeletion in a large kindred with AD-PHP-Ib. Affected individuals from this kindred share an epigenetic defect that is indistinguishable from that observed in patients with AD-PHP-Ib who carry the 3-kb microdeletion in the *STX16* region (i.e., an isolated loss of methylation at *GNAS* exon A/B). The novel 4.4-kb microdeletion overlaps with the previously identified deletion by 1,286 bp and, similar to the latter deletion, removes several exons of *STX16* (encoding syntaxin-16). Because these microdeletions lead to AD-PHP-Ib only after maternal transmission, we analyzed expression of this gene in lymphoblastoid cells of affected individuals with the 3-kb or the 4.4-kb microdeletion, an individual with a NESP55 deletion, and a healthy control. We found that *STX16* mRNA was expressed in all cases from both parental alleles. Thus, *STX16* is apparently not imprinted, and a loss-of-function mutation in one allele is therefore unlikely to be responsible for this disorder. Instead, the region of overlap between the two microdeletions likely harbors a *cis*-acting imprinting control element that is necessary for establishing and/or maintaining methylation at *GNAS* exon A/B, thus allowing normal $G\alpha_s$ expression in the proximal renal tubules. In the presence of either of the two microdeletions, parathyroid hormone resistance appears to develop over time, as documented in an affected individual who was diagnosed at birth with the 4.4-kb deletion of *STX16* and who had normal serum parathyroid hormone levels until the age of 21 mo.

Introduction

GNAS is a complex imprinted locus that yields—in addition to the α-subunit of the stimulatory G protein ($G\alpha_s$)—multiple alternative transcripts (fig. 1). These transcripts encode extra-large $G\alpha_s$ ($XL\alpha_s$) (Kehlenbach et al. 1994; Hayward et al. 1998*a*; Peters et al. 1999) or neurosecretory protein 55 (NESP55) (Ischia et al. 1997; Hayward et al. 1998*b*; Peters et al. 1999), or they lead to presumably nontranslated RNAs, such as the A/B transcript (also referred to as "1A" or "1′") (Ishikawa et al. 1990; Swaroop et al. 1991; Liu et al. 2000*b*) and the antisense (AS) transcript (referred to as "*Nespas*" in mouse) (Hayward and Bonthron 2000; Liu et al. 2000*b*; Wroe et al. 2000). NESP55, $XL\alpha_s$, and A/B differ from $G\alpha_s$ only by their first exons, whereas AS transcripts consist of entirely distinct exons. AS, $XL\alpha_s$, and A/B are paternally derived transcripts, whereas NESP55 is a maternally derived transcript. Consistent with their monoallelic expression, the promoters of these imprinted transcripts are located within differentially methylated regions (DMRs) (fig. 1). In contrast, the promoter that gives rise to $G\alpha_s$ is not methylated, and, accordingly, expression of $G\alpha_s$ occurs in most tissues from both parental *GNAS* alleles (Campbell et al. 1994; Hayward et al. 1998*a*, 1998*b*; Zheng et al. 2001). In some tissues (including proximal renal tubules, pituitary, gonads, and thyroid), however, $G\alpha_s$ transcripts are predominantly derived from the maternal allele (Hayward et al. 1998*a*, 2001; Yu et al. 1998; Li et al. 2000; Mantovani et al. 2002).

Pseudohypoparathyroidism (PHP) is a disorder characterized by hypocalcemia, hyperphosphatemia, and parathyroid hormone (PTH) levels that are elevated as a result of end-organ resistance to this hormone. One of the two main subtypes of PHP, PHP type Ia (PHP-Ia [MIM 103580]), is caused by heterozygous maternally inherited loss-of-function mutations in *GNAS* exons 1–13, which encode $G\alpha_s$. In addition to PTH resistance, affected individuals typically show clinical abnormali-

Received December 30, 2004; accepted for publication February 23, 2005; electronically published March 30, 2005.

Address for correspondence and reprints: Dr. Murat Bastepe, Endocrine Unit, Massachusetts General Hospital, 50 Blossom Street, WEL 5, Boston, MA 02114. E-mail: bastepe@helix.mgh.harvard.edu

0002-9297/2005/7605-0009$15.00

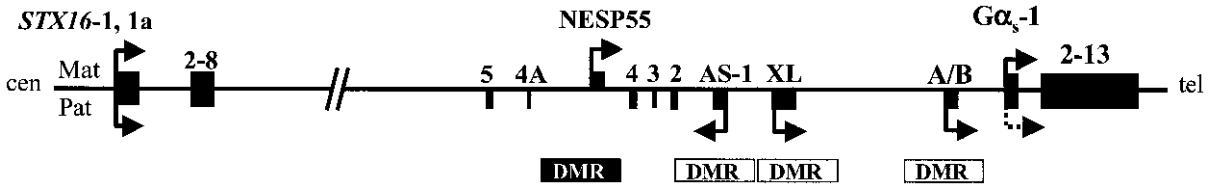

Figure 1 Schematic representation of the human *STX16* and *GNAS* loci (not to scale). Exons are depicted as blackened boxes; arrows indicate direction (sense, antisense) and allelic origin (Mat = maternal [*above the line*]; Pat = paternal [*below the line*]) of transcription. Note that $G\alpha_s$ is transcribed from both alleles in most tissues (Campbell et al. 1994; Hayward et al. 1998*a*, 1998*b*; Zheng et al. 2001) and that the paternal allele is silenced (*dotted arrow*) in some tissues, including kidney, adipose tissue, and pituitary (Hayward et al. 1998*a*, 2001; Yu et al. 1998; Li et al. 2000; Mantovani et al. 2002). Paternal and maternal DMRs are indicated by blackened and unblackened rectangles, respectively.

ties referred to as "Albright hereditary osteodystrophy" (AHO) and resistance toward several additional hormones, including thyroid-stimulating hormone (TSH) and gonadotropins. When inherited paternally, $G\alpha_s$ loss-of-function mutations are associated with AHO alone, in the absence of hormonal resistance—a variant termed "pseudopseudohypoparathyroidism" (PPHP) (Weinstein et al. 2001; Levine 2002). The other main form of PHP, PHP type Ib (PHP-Ib [MIM 603233]), differs from PHP-Ia and PPHP, in that PHP-Ib patients do not have the AHO phenotype (Weinstein et al. 2001). Furthermore, hormone resistance in PHP-Ib appears to be limited to the renal actions of PTH, although resistance to TSH is also seen occasionally (Bastepe et al. 2001*a*, 2001*b*; Liu et al. 2003).

The autosomal dominant variant of PHP-Ib (AD-PHP-Ib) has been linked to a region of chromosome 20q13.3 that comprises the *GNAS* locus, and, similar to PHP-Ia, this disorder is maternally transmitted (Jüppner et al. 1998). Most individuals affected by AD-PHP-Ib show a methylation defect that is limited to *GNAS* exon A/B, whereas most apparently sporadic cases of the disease display abnormal methylation at other *GNAS* DMRs as well (Liu et al. 2000*a*, 2005; Bastepe et al. 2001*b*, 2003). An identical 3-kb microdeletion located ~220 kb upstream of *GNAS* has been identified in all affected members and obligate carriers of 14 unrelated families with AD-PHP-Ib and in two apparently sporadic cases (Bastepe et al. 2003). All affected individuals share the same epigenetic defect at exon A/B and lack methylation abnormalities at the other DMRs of *GNAS*. The 3-kb microdeletion lies between two direct repeats and removes intronic as well as exonic sequences of the gene encoding syntaxin-16 (*STX16*). Consistent with the imprinted inheritance pattern of the disease, transmission of the microdeletion from a female obligate carrier causes PTH resistance, whereas transmission of the same mutation from a male obligate carrier results in normal PTH responsiveness (Bastepe et al. 2003). Recently, additional patients with PHP-Ib and with the isolated *GNAS* exon A/B methylation defect have been reported to carry the same 3-kb microdeletion (Liu et al. 2005; Mahmud et al. 2005), thereby strengthening the likely causative association between the exon A/B methylation defect and this deletion.

In one family with AD-PHP-Ib (kindred W), the 3-kb microdeletion was not found, despite a loss of methylation at *GNAS* exon A/B alone in the affected individuals (Bastepe et al. 2001*b*, 2003), suggesting the presence of another mutation in the *STX16* region. We thus searched, in this family, for mutations within *STX16* and identified a novel microdeletion in all affected members and unaffected carriers.

Subjects and Methods

Kindred W and Methylation Analysis of GNAS *Exon A/B*

The pedigree (kindred W) and the clinical and laboratory data of most members of this family have been described elsewhere (Bastepe et al. 2001*b*) (see also fig. 2*A*). Genomic DNA was isolated from blood leukocytes of all family members, and a lymphoblastoid cell line was established for patient W-III/3 (Harvard-Partners Center for Genetics and Genomics Biosample Services Facility). Written informed consent was obtained from all investigated individuals (Massachusetts General Hospital institutional review board [#2001p-000648]).

Since 2001, when this family was first reported (Bastepe et al. 2001*b*), two children have been born: W-III/12 (born to W-II/9) and W-III/13 (born to W-II/10). Genomic DNA was extracted from cord blood of both children. Methylation of *GNAS* exon A/B was assessed by nucleotide sequence analysis of PCR-amplified bisulfite-treated genomic DNA and by Southern blot analysis with the use of *Eag*I (methylation sensitive) and *Eco*RV (methylation insensitive) (New England Biolabs), as described elsewhere (Jüppner et al. 1998; Bastepe et al. 2001*b*, 2003). Total serum calcium, phosphorus, intact PTH (Nichols Institute), and TSH were measured

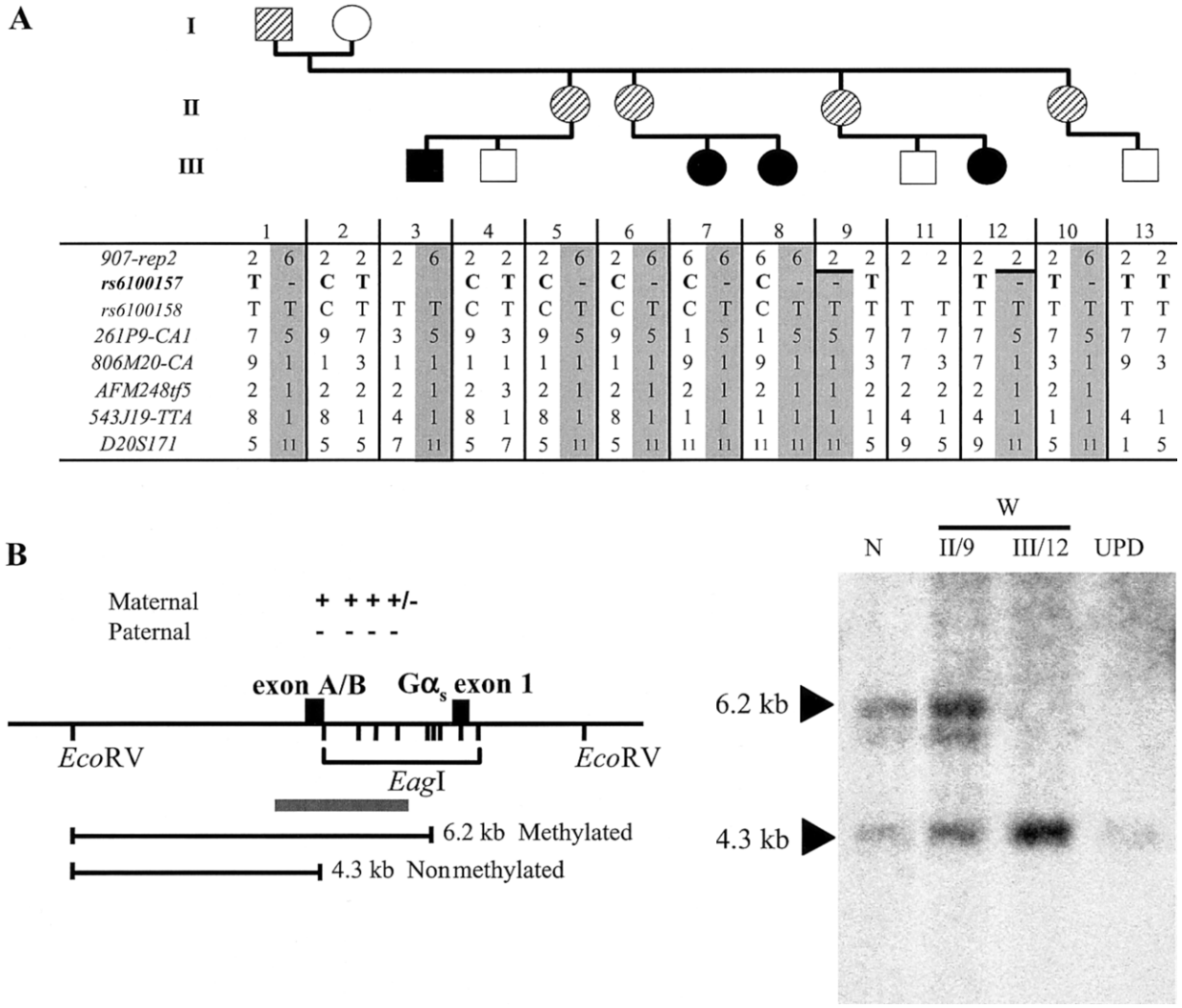

Figure 2 *A*, Evidence of allelic loss within the *STX16* locus in the obligate carriers W-II/5 and W-II/6. All the affected individuals (*blackened symbols*) as well as the obligate carriers (*striped symbols*) share the same disease-associated haplotype (*gray columns*) at 20q13.3; note that not all investigated markers are shown. A recombination event occurred in individual W-II/9 between markers *907-rep2* and *261P9-CA1* and was transmitted to her affected daughter, W-III/12, thus reducing the critical interval likely containing the genetic lesion that causes AD-PHP-Ib. Evidence of allelic loss was found at SNP *rs6100157* (*bold typeface*) in obligate carriers W-II/5 and W-II/6. *B*, Loss of methylation at *GNAS* exon A/B in the newborn W-III/12. The methylation status of *GNAS* exon A/B was assessed by Southern blot analysis of cord blood DNA from patient W-III/12 and of genomic DNA from her unaffected mother (W-II/9), an individual with paternal uniparental isodisomy of chromosome 20q ("UPD") (Bastepe et al. 2001*a*), and a healthy control individual ("N"). These samples were digested with a methylation-sensitive (*Eag*I) and a methylation-insensitive (*Eco*RV) restriction endonuclease, as described elsewhere (Bastepe et al. 2001*b*). Locations of restriction sites and their methylation status ("+" = methylated; "−" = nonmethylated), the predicted fragments, and the probe (*gray bar*) are shown in the left panel. Affected individuals (UPD and W-III/12) show loss of methylation at exon A/B, whereas unaffected individuals (N and W-II/9) have one methylated and one nonmethylated allele. Fragment sizes are indicated by arrowheads. Note that the faint hybridizing band below the 6.2-kb band reflects partial methylation ("+/−") and, hence, incomplete digestion at one of the *Eag*I sites between exon A/B and $G\alpha_s$ exon 1.

in patient W-III/12 shortly after birth and subsequently at regular intervals.

Analysis of Microsatellite Markers and SNPs

Microsatellite markers *D20S102, D20S25, D20S86, D20S164, 907-Rep2, 907-Rep4, 261P9-CA1, 806M20-CA, AFM248tf5, GNAS, 543J19-TTA, D20S171, st-AFMa202yb9,* and *D20S93* were analyzed as described elsewhere (Bastepe et al. 2003). SNPs *rs6100157, rs2296524,* and *rs6100158*—which correspond to nucleotides 3959, 4712, and 5326, respectively, of AL139349—were analyzed by nucleotide sequence anal-

Table 1

Sequences of the Primers Used in the Present Study

The table is available in its entirety in the online edition of *The American Journal of Human Genetics*.

ysis after PCR amplification, which was performed using conditions and primers reported elsewhere (table 1) (Jüppner et al. 1998; Bastepe et al. 2001*b*, 2003).

Southern Blot and PCR Analysis for Detection of the Deletion

For Southern blot analysis, genomic DNA (5 μg) was digested with *Afl*II, *Bcl*I, or *Bgl*II (New England Biolabs). After separation on a 0.8% agarose gel, DNA fragments were transferred onto a nitrocellulose filter and were hybridized with a ^{32}P-radiolabeled probe (nucleotides 8299–9921 of AL139349), which was generated by PCR; primers are listed in table 1.

PCR amplification of genomic DNA across the predicted deletion was performed using primers 5.9 kb apart from each other (primers A and B) (table 1) and the Expand Long-Template PCR System with Buffer 3 (Roche Molecular Biochemicals). The cycling conditions were an initial 94°C for 3 min; 10 cycles of 94°C for 10 s, 58°C for 30 s, and 68°C for 5 min; 25 cycles of 94°C for 10 s, 58°C for 30 s, and 68°C for 5 min, with an additional 20 s at 68°C after each cycle; and 1 final cycle at 72°C for 10 min. These conditions yielded a 5.9-kb amplicon, which was not consistently amplified in all samples. The same conditions also yielded an ~1.5-kb amplicon in affected individuals and obligate carriers, which was gel purified and submitted for nucleotide sequence analysis (Massachusetts General Hospital DNA Core Facility).

For multiplex PCR, two pairs of primers (C and D, E and F) were designed, to amplify small fragments across each boundary of the deletion (table 1). Both pairs were used for simultaneous PCR amplification of three different fragments: a 616-bp fragment (primers C and D) and a 252-bp fragment (primers E and F), derived from the centromeric and telomeric ends of the deleted region, respectively, as well as a 4.8-kb fragment (primers C and F), derived from the wild-type allele. As a result of its large size, however, the latter fragment could not be effectively amplified each time.

Analyzing STX16 *Transcripts*

Total RNA was extracted from lymphoblastoid cells derived from the affected individuals W-III/3, F-III/37, C-II/1, as well as a healthy control individual (Harvard-Partners Center for Genetics and Genomics Biosample Services Facility). Subject F-III/37 carries the previously described 3-kb deletion (Bastepe et al. 2003). Subject C-II/1 has methylation abnormalities at all *GNAS* DMRs and has been recently shown to carry a novel microdeletion involving exon NESP55 and antisense exons 3 and 4 (Bastepe et al. 2005). Consistent with the conclusion that the *STX16* region is intact, subject C-II/1 was furthermore shown to be heterozygous at SNPs *rs6100157* and *rs2296524,* which are located within the centromeric repeat and *STX16* exon 4, respectively. STX16 mRNAs were amplified by RT-PCR. One microgram of lymphoblast-derived total RNA was reverse transcribed using Superscript II (Invitrogen) and oligo (dT) primers, in accordance with manufacturer recommendations; the same reactions, without reverse transcriptase, served as negative controls. PCR was then performed using 1 μl of 1:10 dilution of the reverse-transcription mixture, a forward primer located in exon 1 (primer G), and a reverse primer located in exon 8 (primer H) in a total reaction volume of 50 μl (table 1 and fig. 3). The amplification conditions were an initial 94°C for 2 min; 31 cycles of denaturation at 95°C for 30 s, annealing at 61°C for 30 s, and extension at 72°C for 1 min; and 1 final cycle of extension at 72°C for 10 min. Amplicons were separated on a 2% agarose gel, were purified, and were submitted for nucleotide sequence analysis (Massachusetts General Hospital DNA Core Facility), as described elsewhere (Bastepe et al. 2001*b*). To determine the allelic origin of the STX16 transcripts in the healthy control individual and in subject C-II/1, total RNA was amplified by RT-PCR as described above, and the polymorphic nucleotide at position 527 of STX16 isoform B was analyzed by direct sequence analysis of the amplicon; this corresponds to SNP *rs2296524* (table 1).

Results

Loss of Exon A/B Methylation and Development of PTH Resistance

We have reported elsewhere that affected members of kindred W show a loss of exon A/B methylation without additional epigenetic defects of *GNAS* (Bastepe et al. 2003). Nucleotide sequence analysis of PCR-amplified bisulfite-treated cord blood DNA from the newborn W-III/13 showed a normal methylation pattern at *GNAS* exon A/B (data not shown). Accordingly, haplotype analysis across the *GNAS* region revealed that this individual had inherited the grandmaternal haplotype, which is not associated with disease (fig. 2*A*) (Bastepe et al. 2001*b*). Thus, two independent approaches indicated that subject W-III/13 would not be affected with AD-PHP-Ib. In contrast, Southern blot analysis of cord blood DNA from his cousin, W-III/12, performed using the restriction endonucleases *Eco*RV and *Eag*I, showed loss of methylation at *GNAS* exon A/B (fig. 2*B*), and

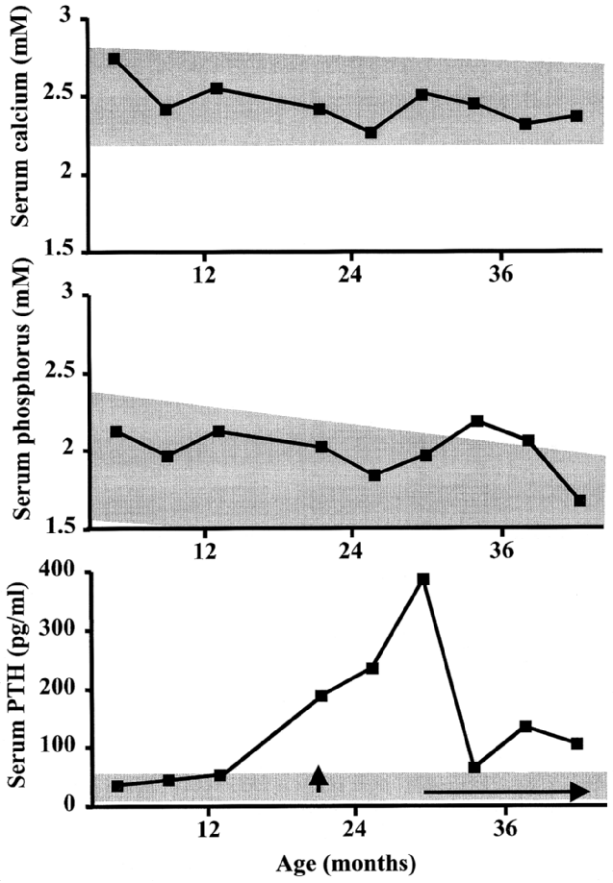

Figure 3 Delayed onset of PTH resistance in patient W-III/12. Serum calcium, phosphorus, and PTH levels were measured during follow-up visits of the patient—in whom loss of methylation at *GNAS* exon A/B was identified at birth—and the 4.4-kb deletion was discovered subsequently. Normal ranges are indicated by gray shading. Treatment with an active vitamin D analog (Rocaltrol) was first started at age 21 mo (*vertical arrow*). However, the parents discontinued the treatment shortly thereafter, and continuous treatment was not resumed until the child was 30 mo old (*horizontal arrow*).

haplotype analysis revealed inheritance of the disease-associated grandpaternal haplotype (fig. 2*A*). She was therefore predicted to develop PTH resistance, which was subsequently documented (see below). Because patient W-III/12 was found to be affected, the maximum LOD score increased from 2.03 (Bastepe et al. 2001*b*) to 2.43 for genetic linkage to 20q13.3 (*D20S171* [$\theta = 0$]), increasing the likelihood that the defect leading to AD-PHP-Ib in this family also resides close to the *GNAS* locus.

Birth weight and height of patient W-III/12 were 4.2 kg (95th percentile [North American reference chart]) and 53 cm (95th percentile), respectively. Her weight, height, and BMI remained above the 95th percentile during infancy and early childhood. Except for being overweight, she had no features suggestive of AHO. PTH resistance was absent at birth but developed by age 21 mo, when serum PTH levels were first noted to be above the normal range (188 pg/ml; normal range 10–65 pg/ml). Both total serum calcium and phosphorous concentrations remained within normal range during this period, although serum phosphorus was close to the upper limit (fig. 3). Because of the genetic findings and the elevation in PTH concentration, treatment with an active vitamin D analog (Rocaltrol) and calcium supplements was first initiated at age 21 mo. However, the parents discontinued these medications shortly thereafter, and it was not until the child was 30 mo old that uninterrupted treatment was started. By that time, the PTH concentration had increased to 386 pg/ml. In addition, mild TSH resistance was suspected at age 30 mo because of elevated TSH (14.5 mUI/l; normal range 0.5–5 mUI/l), normal free T4 (0.9 ng/dl; normal range 0.7–1.7 ng/dl), and undetectable serum anti-thyroglobulin and anti-thioperoxidase antibodies. L-thyroxine treatment was then started, and the TSH level dropped to the normal range (2.89 mUI/l at 41 mo).

Identification of a Novel Deletion within the STX16 *Region*

All affected individuals of kindred W (W-III/3, W-III/7, W-III/8, and W-III/12) showed a loss of methylation at *GNAS* exon A/B, without methylation abnormalities involving the NESP55, XL, or AS DMRs (fig. 2*B* and Bastepe et al. [2001*b*]). Nevertheless, unlike many other kindreds with AD-PHP-Ib with the same epigenetic defect, the previously described 3-kb deletion (nucleotides 3786–6764 of AL139349) could not be found in this kindred. In fact, all affected individuals and obligate carriers were heterozygous at microsatellite marker *261P9-CA1,* and some of them, furthermore, were heterozygous at SNP *rs6100158* (figs. 2*A* and 4*A*). In addition, PCR analysis across the 3-kb deletion, performed using previously established primers and conditions (Bastepe et al. 2003), revealed no evidence of a smaller deletion within this region.

Analysis of additional polymorphisms centromeric of the heterozygous SNP *rs6100158* revealed allelic loss at SNP *rs6100157* for the obligate carriers W-II/5 and W-II/6, indicating the presence of a deletion comprising this region (figs. 2*A* and 4*A*). This deletion was confirmed by Southern blot analysis of genomic DNA from individual W-II/5 and her unaffected child W-III/4, performed using restriction enzymes *Afl*II, *Bcl*I, or *Bgl*II (fig. 4*B*). The probe, located telomeric of SNP *rs6100158,* detected wild-type hybridizing fragments of 7.9 kb, 9.8 kb, and 9.2 kb in both samples. In addition, however, hybridizing *Afl*II, *Bcl*I, and *Bgl*II fragments of ~6.8 kb, 11.1 kb, and 7 kb were detected, respectively, in the DNA sample from individual W-II/5 but not in the DNA

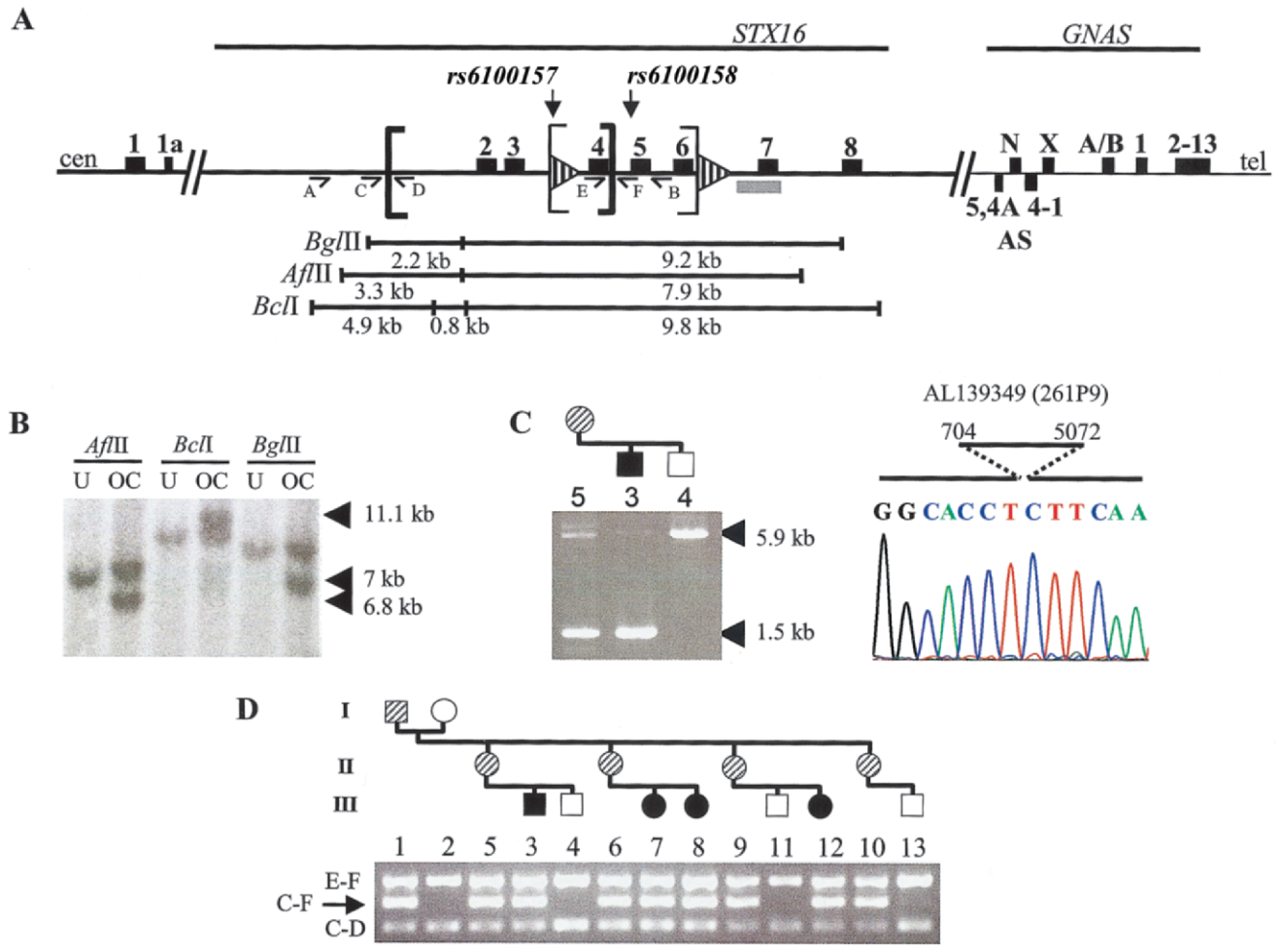

Figure 4 Identification of a novel 4.4-kb deletion in kindred W. *A,* Simplified map of the 20q13.3 region and the localization of the two known microdeletions. Sequence of the depicted region is included in AL050327 (clone 907D15) and AL139349 (clone 261P9). Exons are depicted as blackened rectangles, and direct repeats are shown as striped arrowheads. The 3-kb and 4.4-kb deleted regions lie between the thin and thick brackets, respectively. The locations of recognition sites for the restriction endonucleases used in the Southern blot analysis are shown under the gene map. The location of the 1.6-kb probe is marked by the gray bar, and primers A, B, C, D, E, and F, which were used for PCR analyses, are indicated by arrowed lines; cen = centromeric; tel = telomeric; N = NESP55; AS = antisense; X = XLα_s; A/B = exon A/B. *B,* Southern blot analysis of genomic DNA from an unaffected ("U") subject, W-III/4, and an obligate carrier ("OC"), W-II/5, which was digested with three different restriction endonucleases (*Afl*II, *Bcl*I, and *Bgl*II). Hybridization with the 1.6-kb ^{32}P-labeled probe (nucleotides 8299–9921 of AL139349) showed the expected wild-type bands of 7.9 kb, 9.8 kb, and 9.2 kb, respectively. Additional bands (*arrowheads*) in the obligate carrier (6.8 kb, 11.1 kb, and 7 kb, respectively) are compatible with a 4.4-kb deletion removing one *Afl*II site, two *Bcl*I sites, and one *Bgl*II site—all of which are centromeric of *STX16* exon 2. *C,* Confirmation and exact localization of the deletion by PCR. Amplification across the predicted location of the deletion, performed using one pair of primers (A [forward] and B [reverse]), yielded a 5.9-kb wild-type fragment in the unaffected subject, the affected individual, and the obligate carrier; both the affected individual and the obligate carrier also showed a shorter fragment (of 1.5 kb). Direct nucleotide sequence analysis of the short amplicon revealed the lack of 4,368 bp extending from nucleotide 704 to nucleotide 5072 of AL139349. *D,* Amplification of the *STX16* region with four different primers, located at nucleotides 404 (primer C [forward]), 1020 (primer D [reverse]), 4938 (primer E [forward]), and 5190 (primer F [reverse]) of AL139349. The sizes of expected wild-type PCR products are 616 bp (primers C and D), 252 bp (primers E and F), and 4.8 kb (primers C and F [not shown]). Obligate carriers and affected individuals show an additional 422-bp amplicon (*arrow* [primers C and F]). Results are shown for each individual in the family (blackened symbols represent affected individuals, striped symbols represent obligate carriers, and unblackened symbols represent unaffected individuals).

sample from individual W-III/4. The sizes of these additional bands were compatible with an ~4.4-kb deletion that removed one centromeric *Afl*II site, two *Bcl*I sites, and one *Bgl*II site.

To determine the exact location of the deletion, we performed a series of PCRs with the use of primers that were predicted to amplify a region of the mutant allele spanning the deletion breakpoint. One set of primers (primers A and B) amplified a single product of ~5.9 kb from genomic DNA of the unaffected individual W-III/4, whereas the same primers produced an additional smaller amplicon of ~1.5 kb from DNA of the affected individual W-III/3 and unaffected carrier W-II/5 (fig. 4*A* and 4*C*). The difference between the lengths of the small and the large amplicons was consistent with a 4.4-kb deletion, suggesting that the small amplicon was derived from the mutant allele. Direct nucleotide sequence analysis of this mutant fragment showed that the deletion occurred between nucleotides 704 and 5072 of AL139349, thus eliminating exons 2–4 of *STX16* (fig. 4*C*). The presence of this deletion was also confirmed in the remaining affected individuals or unaffected carriers by multiplex PCR, performed using primers designed to amplify across the deleted region and across the predicted boundaries. All affected individuals and obligate carriers of kindred W showed—in addition to the wild-type products of 616 bp (primers C and D) and 252 bp (primers E and F)—a 422-bp product amplified across the deletion breakpoints (primers C and F) (fig. 4*A* and 4*D*). In contrast, genomic DNA from the healthy individuals generated only the two wild-type fragments; note that the 4.8-kb product derived from the wild-type allele (primers C and F) could not be routinely amplified, because of its size (data not shown).

Biallelic Expression of STX16

Although the identified deletion removes coding exons from the gene *STX16,* a loss-of-function mutation in one *STX16* allele could not directly explain the imprinted AD-PHP-Ib phenotype unless *STX16* itself is an imprinted gene. We therefore examined allelic expression of *STX16* in total RNA extracted from lymphoblastoid cells of a healthy control individual and of three AD-PHP-Ib individuals carrying different mutations. *STX16* normally gives rise to at least three differently spliced mRNA transcripts: STX16A, STX16B, and STX16C (AL050327 and AL139349 [fig. 5*A*]). RT-PCR amplification of total RNA from both the control individual and subject C-II/1 (deletion of the NESP55 DMR [Bastepe et al. 2005]), performed using primers G and H, yielded products of 861 bp and 802 bp, corresponding to isoform B of STX16 and its splice variant (which is missing the alternatively spliced exon 4), respectively (fig. 5*B*). Subsequent nucleotide sequence analysis of the 861-bp products revealed heterozygosity at position 527 of STX16 isoform B located within exon 4 (SNP *rs2296524* [fig. 5*C*]), indicating that both parental alleles were transcribed and amplified. Furthermore, RT-PCR performed using lymphoblast-derived total RNA of the affected individual W-III/3 (4.4-kb *STX16* deletion) showed amplicons from the wild-type splice variants of STX16 isoform B, as well as a shorter amplicon of 449 bp (fig. 5*A* and 5*B*). Direct sequence analysis of this short product confirmed the absence of nucleotides derived from *STX16* exons 2, 3, and 4. Likewise, transcripts amplified by RT-PCR from individual F-III/37 (3-kb *STX16* deletion) included, in addition to the wild-type splice variants of STX16 isoform B, a shortened transcript represented by an amplicon of 462 bp (fig. 5*A* and 5*B*). Nucleotide sequence analysis of this shorter product confirmed the deletion of exons 4, 5, and 6. Together, these findings suggested that both parental *STX16* alleles are transcribed in lymphoblastoid cells and that the identified deletions do not appear to alter this biallelic expression. We also searched the EST database and identified two ESTs (CN348556 and CN417685) matching the *STX16* exon 8 sequence that were derived from the same cDNA library yet differed by one nucleotide (position 937 of STX16 isoform B; position 11538 of AL139349). Since this nucleotide change was also seen in several other ESTs from the database, it indicated its polymorphic nature rather than a sequence error. This finding strongly suggested that STX16 mRNAs were amplified from both parental alleles in that particular library as well.

Discussion

We report a novel *STX16* microdeletion of 4.4 kb in all affected individuals and obligate carriers of a large kindred with AD-PHP-Ib. This 4.4-kb microdeletion was present in the unaffected mothers of the affected individuals ($n = 4$) and in the father of these obligate carriers (figs. 2 and 4). This mode of inheritance is concordant with the paternal imprinting of the disease in this and other families with AD-PHP-Ib. The 4.4-kb microdeletion is the first *STX16* mutation identified in patients with AD-PHP-Ib that differs from the 3-kb microdeletion present in multiple unrelated kindreds with this disorder (Bastepe et al. 2003; Liu et al. 2005; Mahmud et al. 2005). Our findings thus provide further evidence supporting the conclusion that *STX16* harbors an important element involved in the pathogenesis of PHP-Ib. As the two deletions overlap by 1,286 bp, it is likely that this element is contained in this overlap region. Thus far, of the 31 unrelated individuals with PHP-Ib that we have investigated, 18 (58%) carry a deletion within *STX16* (Bastepe et al. 2003; Mahmud et al. 2005). Recently, the 3-kb deletion has also been found

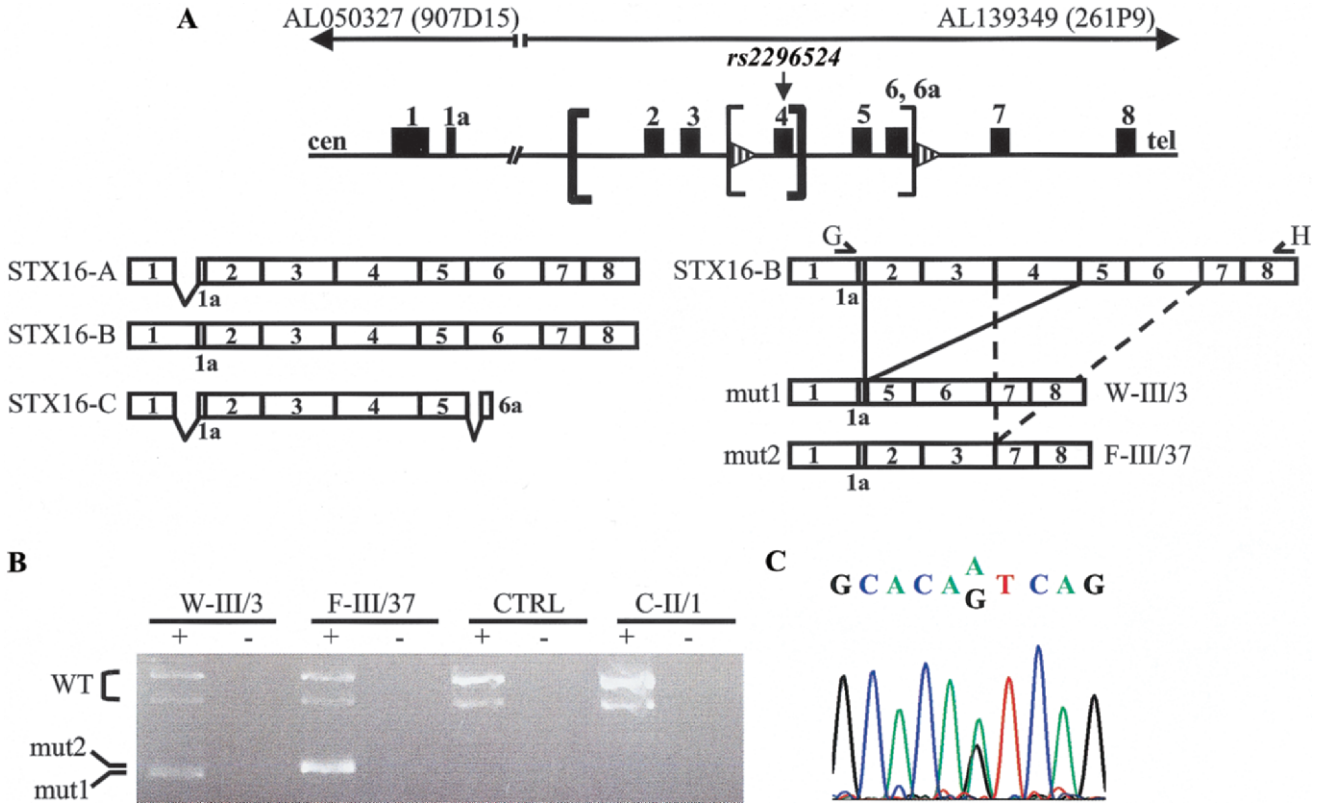

Figure 5 Biallelic expression of *STX16*. *A*, *STX16* gives rise to at least three distinct transcripts (*left*). Isoform A (915 bp) differs from isoform B (965 bp) by a shorter sequence derived from exon 1, whereas isoform C (422 bp) comprises this short exon 1 sequence as well as exons 2–5 and terminates with exon 6a. In addition, exon 4 is alternatively spliced in each isoform, leading to a total of at least six variants. Wild-type STX16 isoform B and the transcripts derived from individuals W-III/3 and F-III/37 ("mut1" and "mut2," respectively) are depicted (*right*). The 4.4-kb deletion (*thick brackets*) removes exons 2–4; the 3-kb deletion (*thin brackets*) removes exons 4–6. Exons are depicted as blackened boxes, and direct repeats are shown as striped arrowheads. Primers G and H are represented as arrowed lines; cen = centromeric; tel = telomeric. *B*, RT-PCR analysis of STX16 transcripts in total RNA of immortalized lymphocytes from a healthy control individual (CTRL) and the following individuals with AD-PHP-Ib: W-III/3 (present study), F-III/37 (carrying the 3-kb deletion in *STX16* region [Bastepe et al. 2003]), and C-II/1 (carrying a deletion affecting NESP55 but not the *STX16* region [Bastepe et al. 2005]). Reactions were performed with ("+") or without ("−") reverse transcriptase, as described in the "Subjects and Methods" section. Products derived from the mutant alleles ("mut1" and "mut2") and from the wild-type alleles ("WT") are indicated. Note that the wild-type products represent STX16 isoform B with or without sequences derived from exon 4. *C*, Direct nucleotide sequence of STX16 isoform B amplified from RNA of a healthy control individual shows heterozygosity at the polymorphic nucleotide 527, corresponding to SNP *rs2296524*.

in 5 of 20 unrelated individuals with PHP-Ib (Liu et al. 2005). Thus, mutations in this region are frequently the cause of PHP-Ib. Affected individuals who carry the 3-kb and 4.4-kb microdeletions exhibit loss of methylation only at *GNAS* exon A/B; the methylation pattern is not altered at other *GNAS* DMRs. Conversely, individuals with PHP-Ib who lack such *STX16* deletions display methylation abnormalities at all *GNAS* DMRs (Bastepe et al. 2003; Liu et al. 2005). On the basis of these findings, we conclude that PHP-Ib comprises at least two distinct conditions sharing the same clinical phenotype: one is associated with the loss of exon A/B methylation alone—and, in most of the cases, with a heterozygous microdeletion in the *STX16* region—and the other is associated with methylation abnormalities at all *GNAS* DMRs, including the DMR at exon A/B. In two unrelated kindreds with AD-PHP-Ib with broad methylation defects of *GNAS*, we have recently identified deletions affecting the NESP55 DMR (Bastepe et al. 2005), and it remains to be determined whether the sporadic cases with this epigenotype also carry an as-yet-undefined microdeletion within or close to this region.

Deletion of *STX16* exons 2–4, caused by the mutation presented in the present study, results in a frameshift and a premature termination codon following 20 new amino acids, whereas deletion of *STX16* exons 4–6, caused by the previously described 3-kb microdeletion (Bastepe et al. 2003), maintains the ORF. Thus, the syntaxin-16 proteins generated by the 4.4-kb or 3-kb deleted alleles either are shortened by 276 amino acids

at the carboxyl-terminus or have a deletion of 133 amino acids in the midportion, respectively. Because of these severe alterations, both products are predicted to be nonfunctional, raising the question of whether syntaxin-16 deficiency may be responsible for the epigenetic abnormality at *GNAS* exon A/B and the resulting PTH resistance. However, this possibility seems unlikely for two reasons. First, the previously reported lack of differential methylation at the *STX16* promoter (Bastepe et al. 2003)—as well as our present demonstration of biallelic expression of STX16 isoform B—strongly argues that this gene is not imprinted. Although not entirely ruled out by our analysis, selective imprinting of the other STX16 transcripts seems unlikely, given that all the known transcripts apparently use the same promoter. This lack of parental origin–specific STX16 expression is inconsistent with the imprinted mode of inheritance in kindreds with AD-PHP-Ib. Second, PTH resistance can develop despite the presence of two intact copies of *STX16,* as shown in a case of paternal uniparental isodisomy of chromosome 20q (Bastepe et al. 2001*a*). On the other hand, maternal inheritance of *STX16* mutations is associated with loss of methylation at maternal *GNAS* exon A/B, and it is therefore more likely that these deletions disrupt a *cis*-acting imprinting control element (ICE) necessary for the methylation imprint at exon A/B.

The novel 4.4-kb microdeletion overlaps with the former 3-kb deletion and therefore reduces the size of the critical region containing the putative ICE for *GNAS* exon A/B to 1,286 bp. This region encompasses the centromeric direct repeat, and the flanking telomeric sequence of 896 bp, which includes exon 4 of *STX16* and intronic sequences of 244 bp and 344 bp on the centromeric and telomeric side, respectively. We could not identify, within the 1,286-bp overlapping region, sequences or elements homologous to those previously identified in other ICEs. For example, microdeletions at the ICE of the *IGF2/H19* locus abolish two CTCF binding sites required for the *H19* DMR and thus result in the Beckwith-Wiedemann syndrome (Sparago et al. 2004). Sequence analysis of the overlapping region encompassing exon 4 of *STX16* did not reveal such known CTCF sites. Another feature of ICEs is that they are mostly located within CpG-rich sequences; in addition, they display differential methylation (Spahn and Barlow 2003). Although the overlapping region includes a 140-bp CpG-rich sequence within exon 4 (nucleotides 4572–4711 of AL139349), we have shown elsewhere that this region is not differentially methylated (Bastepe et al. 2003). It is therefore possible that the mechanisms governing the function of the identified ICE are different from those of most other ICEs in the genome (Spahn and Barlow 2003). Further investigations are necessary to identify the specific features required for the proper activity of the putative ICE.

Two candidate ICEs have been previously identified in the mouse *Gnas* cluster: one comprising exon 1A (homolog of human A/B) and the other comprising the *Gnasxl* (homolog of human XLα_s) and *Nespas* promoters (Liu et al. 2000*b*; Coombes et al. 2003). Mice with a paternal ablation of exon 1A exhibit loss of Gα_s silencing in *cis,* leading to expression of the Gα_s transcript from the paternal allele in brown fat and renal proximal tubules (Williamson et al. 2004)—two tissues in which Gα_s is normally expressed from the maternal allele alone (Yu et al. 1998). This ablation does not alter the imprinting of the other alternative transcripts, and it therefore appears that a *cis*-acting element at exon 1A specifically regulates Gα_s expression in brown fat, kidney, and perhaps other tissues. Findings in patients with PHP-Ib indicate that this element allows active transcription from the Gα_s promoter in the kidney only when it is methylated (Liu et al. 2000*a*; Bastepe et al. 2001*b*). However, although the impact of this element is confined to certain tissues, its methylation on the maternal *GNAS* allele appears to be ubiquitous (Liu et al. 2000*b*). Our findings in patients with AD-PHP-Ib provide evidence of another *cis*-acting element within the overlapping region encompassing *STX16* exon 4. The latter appears to specifically control the methylation of *GNAS* exon A/B and, thus, of the *cis*-acting element regulating the tissue- and parent-specific expression of Gα_s. Deletion of this putative *STX16* ICE results in a switch from a maternal to a paternal epigenotype at exon A/B, thereby causing derepression of maternal A/B transcription. Because the epigenetic changes associated with the deletion of this putative element have been identified in lymphocytes, its impact seems ubiquitous rather than restricted to kidney and brown fat. In addition to this putative ICE that controls methylation on a restricted area of *GNAS* (i.e., exon A/B), the identification of deletions of the NESP55 DMR in two unrelated families with AD-PHP-Ib has recently provided evidence of an additional ICE that is involved in methylation of the entire *GNAS* cluster (Bastepe et al. 2005). Thus, in humans, maternal methylation at *GNAS* exon A/B (and, hence, Gα_s transcription) requires at least two ICEs: one at the *STX16* locus, which affects exon A/B, and the other at the NESP55 DMR, which affects all the maternally methylated promoters within the *GNAS* cluster.

Genetic analysis of cord blood (i.e., exon A/B methylation analysis and multiplex PCR) was particularly useful, allowing us to rule out the diagnosis of AD-PHP-Ib in one newborn and to establish the diagnosis in another. The child with the genetic diagnosis of AD-PHP-Ib was subsequently monitored with respect to development of PTH resistance, and treatment eventually

was started to prevent hypocalcemia and to avoid long-term elevation of serum PTH; the latter can lead to increased bone resorption, resulting from the apparent absence of PTH resistance in this tissue. The observed delay in the onset of PTH resistance in this patient is consistent with past studies of individuals affected with PHP-Ib (Marguet et al. 1997; Bastepe et al. 2001*b*) and was also noted in patients with loss-of-function mutations of $G\alpha_s$ (i.e., PHP-Ia) (Weinstein et al. 2001). PTH signaling through the PTH/PTHrP receptor, therefore, seems intact in the renal proximal tubule during the early postnatal period and infancy. One could hypothesize that $G\alpha_s$ is biallelically expressed in this tissue during this specific period of development. Consistent with this hypothesis, biallelic expression of $G\alpha_s$ has been shown by RT-PCR in whole kidneys and renal cortices from mouse and human fetuses (Hayward et al. 1998*a*; Zheng et al. 2001). However, these findings—which contradict those showing the exclusive maternal expression of $G\alpha_s$ in renal cortices of adult mice (Yu et al. 1998)—do not rule out the possibility that $G\alpha_s$ expression is monoallelic in renal proximal tubules of fetal or newborn kidney, especially considering that proximal tubules constitute a small portion of the entire kidney. Thus, there may be alternative possibilities to explain the delay in the onset of PTH resistance. One of those possible explanations may involve $XL\alpha_s$, the paternally expressed variant of $G\alpha_s$. $XL\alpha_s$ is expressed in multiple fetal and adult tissues (Kehlenbach et al. 1994; Pasolli et al. 2000), including murine kidney at postnatal day 4 (Plagge et al. 2004). Furthermore, on the basis of data from transfected cells lacking endogenous $G\alpha_s$ and $XL\alpha_s$, $XL\alpha_s$ is capable of functionally coupling to the PTH/PTHrP receptor (Bastepe et al. 2002). It is thus possible that PTH actions during early postnatal period are mediated through $XL\alpha_s$.

In conclusion, in the present study, we have (1) identified a novel deletion in the *STX16* locus as a cause of AD-PHP-Ib and therefore established a strong association between a unique epigenotype (i.e., loss of A/B methylation alone) and a genotype (i.e., microdeletion involving *STX16*), (2) refined the boundaries of a putative *cis*-acting ICE crucial for the establishment/maintenance of methylation at *GNAS* exon A/B, (3) demonstrated biallelic expression of STX16 mRNAs in lymphoblastoid cells, and (4) established a molecular diagnosis that was based on cord blood DNA in a patient, which helped in the subsequent clinical management of that patient.

Acknowledgments

This work was supported by grants from National Institutes of Health National Institute of Diabetes and Digestive and Kidney Diseases (RO1 46718-10 [to H.J.] and KO1 DK-062973-01 [to M.B.]) and by a Research Fellowship Grant from the European Society for Paediatric Endocrinology (to A.L.).

Electronic-Database Information

The URL for data presented herein is as follows:

Online Mendelian Inheritance in Man (OMIM), http://www.ncbi.nlm.nih.gov/Omim/

References

Bastepe M, Fröhlich LF, Hendy GN, Indridason OS, Josse RG, Koshiyama H, Korkko J, Nakamoto JM, Rosenbloom AL, Slyper AH, Sugimoto T, Tsatsoulis A, Crawford JD, Jüppner H (2003) Autosomal dominant pseudohypoparathyroidism type Ib is associated with a heterozygous microdeletion that likely disrupts a putative imprinting control element of *GNAS*. J Clin Invest 112:1255–1263

Bastepe M, Fröhlich LF, Linglart A, Abu-Zahra HS, Tojo K, Ward LM, Jüppner H (2005) Deletion of the NESP55 differentially methylated region causes loss of maternal *GNAS* imprints and pseudohypoparathyroidism type Ib. Nat Genet 37:25–27

Bastepe M, Gunes Y, Perez-Villamil B, Hunzelman J, Weinstein LS, Jüppner H (2002) Receptor-mediated adenylyl cyclase activation through XLαs, the extra-large variant of the stimulatory G protein α-subunit. Mol Endocrinol 16:1912–1919

Bastepe M, Lane AH, Jüppner H (2001*a*) Paternal uniparental isodisomy of chromosome 20q—and the resulting changes in *GNAS1* methylation—as a plausible cause of pseudohypoparathyroidism. Am J Hum Genet 68:1283–1289

Bastepe M, Pincus JE, Sugimoto T, Tojo K, Kanatani M, Azuma Y, Kruse K, Rosenbloom AL, Koshiyama H, Jüppner H (2001*b*) Positional dissociation between the genetic mutation responsible for pseudohypoparathyroidism type Ib and the associated methylation defect at exon A/B: evidence for a long-range regulatory element within the imprinted *GNAS1* locus. Hum Mol Genet 10:1231–1241

Campbell R, Gosden CM, Bonthron DT (1994) Parental origin of transcription from the human *GNAS1* gene. J Med Genet 31:607–614

Coombes C, Arnaud P, Gordon E, Dean W, Coar EA, Williamson CM, Feil R, Peters J, Kelsey G (2003) Epigenetic properties and identification of an imprint mark in the Nesp-Gnasxl domain of the mouse *Gnas* imprinted locus. Mol Cell Biol 23:5475–5488

Hayward B, Barlier A, Korbonits M, Grossman A, Jacquet P, Enjalbert A, Bonthron D (2001) Imprinting of the $G_s\alpha$ gene *GNAS1* in the pathogenesis of acromegaly. J Clin Invest 107: R31–R36

Hayward B, Bonthron D (2000) An imprinted antisense transcript at the human *GNAS1* locus. Hum Mol Genet 9:835–841

Hayward B, Kamiya M, Strain L, Moran V, Campbell R, Hayashizaki Y, Bonthron DT (1998*a*) The human *GNAS1* gene is imprinted and encodes distinct paternally and biallelically expressed G proteins. Proc Natl Acad Sci USA 95:10038–10043

Hayward BE, Moran V, Strain L, Bonthron DT (1998*b*) Bi-

directional imprinting of a single gene: *GNAS1* encodes maternally, paternally, and biallelically derived proteins. Proc Natl Acad Sci USA 95:15475–15480

Ischia R, Lovisetti-Scamihorn P, Hogue-Angeletti R, Wolkersdorfer M, Winkler H, Fischer-Colbrie R (1997) Molecular cloning and characterization of NESP55, a novel chromogranin-like precursor of a peptide with 5-HT1B receptor antagonist activity. J Biol Chem 272:11657–11662

Ishikawa Y, Bianchi C, Nadal-Ginard B, Homcy CJ (1990) Alternative promoter and 5′ exon generate a novel $G_s\alpha$ mRNA. J Biol Chem 265:8458–8462

Jüppner H, Schipani E, Bastepe M, Cole DEC, Lawson ML, Mannstadt M, Hendy GN, Plotkin H, Koshiyama H, Koh T, Crawford JD, Olsen BR, Vikkula M (1998) The gene responsible for pseudohypoparathyroidism type Ib is paternally imprinted and maps in four unrelated kindreds to chromosome 20q13.3. Proc Natl Acad Sci USA 95:11798–11803

Kehlenbach RH, Matthey J, Huttner WB (1994) XLαs is a new type of G protein. Nature 372:804–809 (erratum 375: 253)

Levine MA (2002) Pseudohypoparathyroidism. In: Bilezikian JP, Raisz LG, Rodan GA (eds) Principles of bone biology. Vol 2. Academic Press, New York, pp 1137–1163

Li T, Vu TH, Zeng ZL, Nguyen BT, Hayward BE, Bonthron DT, Hu JF, Hoffman AR (2000) Tissue-specific expression of antisense and sense transcripts at the imprinted *Gnas* locus. Genomics 69:295–304

Liu J, Erlichman B, Weinstein LS (2003) The stimulatory G protein α-subunit Gsα is imprinted in human thyroid glands: implications for thyroid function in pseudohypoparathyroidism types Ia and Ib. J Clin Endocrinol Metab 88:4336–4341

Liu J, Litman D, Rosenberg M, Yu S, Biesecker L, Weinstein L (2000*a*) A *GNAS1* imprinting defect in pseudohypoparathyroidism type Ib. J Clin Invest 106:1167–1174

Liu J, Nealon JG, Weinstein LS (2005) Distinct patterns of abnormal *GNAS* imprinting in familial and sporadic pseudohypoparathyroidism type Ib. Hum Mol Genet 14:95–102

Liu J, Yu S, Litman D, Chen W, Weinstein L (2000*b*) Identification of a methylation imprint mark within the mouse *gnas* locus. Mol Cell Biol 20:5808–5817

Mahmud FH, Linglart A, Bastepe M, Jüppner H, Lteif AN (2005) Molecular diagnosis of pseudohypoparathyroidism type Ib in a family with presumed paroxysmal dyskinesia. Pediatrics 115:e242–e244

Mantovani G, Ballare E, Giammona E, Beck-Peccoz P, Spada A (2002) The Gsα gene: predominant maternal origin of transcription in human thyroid gland and gonads. J Clin Endocrinol Metab 87:4736–4740

Marguet C, Mallet E, Basuyau JP, Martin D, Leroy M, Brunelle P (1997) Clinical and biological heterogeneity in pseudohypoparathyroidism syndrome: results of a multicenter study. Horm Res 48:120–130

Pasolli H, Klemke M, Kehlenbach R, Wang Y, Huttner W (2000) Characterization of the extra-large G protein α-subunit XLαs. I. Tissue distribution and subcellular localization. J Biol Chem 275:33622–33632

Peters J, Wroe SF, Wells CA, Miller HJ, Bodle D, Beechey CV, Williamson CM, Kelsey G (1999) A cluster of oppositely imprinted transcripts at the *Gnas* locus in the distal imprinting region of mouse chromosome 2. Proc Natl Acad Sci USA 96: 3830–3835

Plagge A, Gordon E, Dean W, Boiani R, Cinti S, Peters J, Kelsey G (2004) The imprinted signaling protein XLαs is required for postnatal adaptation to feeding. Nat Genet 36:818–826

Spahn L, Barlow DP (2003) An ICE pattern crystallizes. Nat Genet 35:11–12

Sparago A, Cerrato F, Vernucci M, Ferrero GB, Silengo MC, Riccio A (2004) Microdeletions in the human H19 DMR result in loss of *IGF2* imprinting and Beckwith-Wiedemann syndrome. Nat Genet 36:958–960

Swaroop A, Agarwal N, Gruen JR, Bick D, Weissman SM (1991) Differential expression of novel Gsα signal transduction protein cDNA species. Nucleic Acids Res 19:4725–4729

Weinstein LS, Yu S, Warner DR, Liu J (2001) Endocrine manifestations of stimulatory G protein α-subunit mutations and the role of genomic imprinting. Endocr Rev 22:675–705

Williamson CM, Ball ST, Nottingham WT, Skinner JA, Plagge A, Turner MD, Powles N, Hough T, Papworth D, Fraser WD, Maconochie M, Peters J (2004) A cis-acting control region is required exclusively for the tissue-specific imprinting of *Gnas*. Nat Genet 36:894–899

Wroe SF, Kelsey G, Skinner JA, Bodle D, Ball ST, Beechey CV, Peters J, Williamson CM (2000) An imprinted transcript, antisense to Nesp, adds complexity to the cluster of imprinted genes at the mouse *Gnas* locus. Proc Natl Acad Sci USA 97: 3342–3346

Yu S, Yu D, Lee E, Eckhaus M, Lee R, Corria Z, Accili D, Westphal H, Weinstein LS (1998) Variable and tissue-specific hormone resistance in heterotrimeric G_s protein α-subunit ($G_s\alpha$) knockout mice is due to tissue-specific imprinting of the $G_s\alpha$ gene. Proc Natl Acad Sci USA 95:8715–8720

Zheng H, Radeva G, McCann JA, Hendy GN, Goodyer CG (2001) Gαs transcripts are biallelically expressed in the human kidney cortex: implications for pseudohypoparathyroidism type Ib. J Clin Endocrinol Metab 86:4627–4629